



HAL
open science

Holocene vegetation, climate and fire dynamics in the Serra dos Órgãos, Rio de Janeiro State, southeastern Brazil

Maria Carolina Guarinello de Oliveira Portes, Hermann Behling, Vincent Montade, Hugh Deforest Safford

► **To cite this version:**

Maria Carolina Guarinello de Oliveira Portes, Hermann Behling, Vincent Montade, Hugh Deforest Safford. Holocene vegetation, climate and fire dynamics in the Serra dos Órgãos, Rio de Janeiro State, southeastern Brazil. *Acta Palaeobotanica*, 2020, 60 (2), pp.438-453. 10.35535/acpa-2020-0019 . hal-03445331

HAL Id: hal-03445331

<https://hal.science/hal-03445331v1>

Submitted on 23 Nov 2021

HAL is a multi-disciplinary open access archive for the deposit and dissemination of scientific research documents, whether they are published or not. The documents may come from teaching and research institutions in France or abroad, or from public or private research centers.

L'archive ouverte pluridisciplinaire **HAL**, est destinée au dépôt et à la diffusion de documents scientifiques de niveau recherche, publiés ou non, émanant des établissements d'enseignement et de recherche français ou étrangers, des laboratoires publics ou privés.

1 **HOLOCENE VEGETATION, CLIMATE AND FIRE DYNAMICS IN THE SERRA DOS**
2 **ÓRGÃOS, RIO DE JANEIRO STATE, SOUTHEASTERN BRAZIL**

3

4 Maria Carolina Guarinello de Oliveira Portes^{a,b,c,*}; Hermann Behling^a, Vincent Montade^{a,d}, Hugh
5 Deforest Safford^{e,f}

6

7 ^a *University of Goettingen, Department of Palynology and Climate Dynamics, Albrecht-von-*
8 *Haller Institute for Plant Sciences, Germany*

9 ^b *Instituto Chico Mendes de Conservação de Biodiversidade (ICMBio), Brazil*

10 ^c *CNPq-Brazil Scholarship, Brazil*

11 ^d *Université de Montpellier, Institut des Sciences de l'Evolution de Montpellier, CNRS, IRD,*
12 *EPHE, France*

13 ^e *USDA Forest Service, Pacific Southwest Region, Vallejo, California,*

14 ^f *USA Department of Environmental Science and Policy, University of California, Davis,*
15 *California, USA*

16

17 **ABSTRACT** We analysed pollen and macro-charcoal from a sediment core representing the last
18 9840 cal yr BP, collected at 2003 m a.s.l. in a patch of upper montane Atlantic Rain Forest
19 (UMARF) embedded in a campos de altitude (high elevation grassland) matrix in the Serra dos
20 Órgãos National Park, southeastern Brazil. From 9840 to 4480 cal yr BP, campos de altitude
21 (CDA) was the dominant vegetation at the site, indicating that the climate was relatively cool and
22 dry. However, pollen data document that UMARF was near the core site throughout the recorded
23 Holocene. Frequent and high magnitude fires occurred during the Early Holocene but became
24 rarer in the Mid-Holocene after 4480 cal yr BP, when the climate became wetter. In the Mid-
25 Holocene, UMARF and tree fern taxa became slightly more frequent at the site, but CDA
26 vegetation continued to dominate most of the high mountain landscape. A climatic change to
27 wetter and warmer conditions during the last 1350 cal yr BP is evidenced by an increase in
28 UMARF and even lowland forest taxa in our core, as well as the near complete absence of fire
29 after this date.

30 **Key words:** Southeastern Brazil, campos de altitude (high elevation grassland), upper montane
31 Atlantic Rain Forest, climate and fire history, Holocene.

32 INTRODUCTION

33 The Brazilian coastal highlands (Serra do Mar) extend for *c.* 1000 km along the Brazilian
34 coastline from southern to northeastern Brazil, from the north of Santa Catarina State (26° S) to
35 the north of Rio de Janeiro State (21° S) in the Atlantic Forest domain. The Atlantic Forest is one
36 of the world's great tropical forest biomes, and once covered around 130 million ha of coastal
37 and eastern Brazil, stretching *c.* 4000 km from 3° N latitude to almost 34° S (Ribeiro et al., 2009;
38 Fundação SOS Mata Atlântica/ INPE, 2017). Due to the variability of environmental conditions
39 (geomorphology/topography, geology, climate, soils, ecosystems) together with a large
40 elevational range, the Atlantic Forest is one of the most diverse biomes in the world and is
41 considered among the most important and most imperilled biodiversity hotspots on earth (Myers
42 et al., 2000). Before European settlement, the Serra do Mar was clothed in dense rainforest for
43 much of its length, with drier cerrado (Brazilian savanna) formations inland, and elfin “cloud
44 forests” and orographic grasslands (campos de altitude) at higher elevations, mostly above 1500-
45 1800 m a.s.l. (Hueck, 1966; Dean, 1995; Câmara, 2003). At the highest elevations, cloud forests
46 (here referred to as “upper montane Atlantic Rain Forest”, or UMARF) tend to occupy
47 topographic concavities and other protected sites such as valleys and mild slopes, and campos de
48 altitude (CDA) are more common on hilltops, plains, and convex slopes, or where waterlogging
49 occurs (Safford, 1999a).

50 Climatic changes during the Late Quaternary greatly influenced the modern vegetation
51 distribution. Present-day CDA is a vestigial vegetation type from colder and drier climates which
52 reached its widest distribution during the Last Glacial and in particular the Last Glacial
53 Maximum (25,000-17,000 yr BP) when forest vegetation was nearly completely absent in the
54 higher mountains (Behling, 1997b; Behling and Safford, 2010). UMARF expansion began
55 during the Late-glacial, indicating a shift to moister conditions (Behling, 1997b; Behling and
56 Safford, 2010; Ledru et al., 2005; Ledru et al. 2009; Veríssimo et al., 2012). A further increase in
57 both temperature and precipitation in the Early to Mid-Holocene allowed the expansion of the
58 Atlantic Rain Forest to higher elevations, markedly reducing the area occupied by CDA (Behling
59 and Safford, 2010). Displacement of the Intertropical Convergence Zone (ITCZ) over
60 northeastern Brazil might explain the Younger Dryas (YD) warming (second part of the YD
61 period) documented in eastern Brazil, in contrast to the YD cooling in the North Hemisphere
62 (Behling and Safford, 2010). A palaeoecological study carried out by Behling and Safford (2010)

63 at 2130 m elevation in the Serra dos Órgãos (SDO core; Fig. 1c) recorded widespread CDA
64 vegetation and drier climatic conditions until about 5600 cal yr BP. Thereafter a trend toward
65 warmer and wetter conditions resulted in expansion of montane forest and contraction of
66 campos. The last *c.* 1000 years were the wettest period during the whole Holocene (Behling and
67 Safford, 2010).

68 Centuries of exploitation reduced the Atlantic Forest to a patchwork of small fragments in a
69 natural or semi-natural state, covering today only *c.* 10% of its pre-Columbian area (Fundação
70 SOS Mata Atlântica/ INPE, 2017). While more intense occupation and deforestation occurred
71 after European colonization, starting *c.* 1500 AD, the history of human presence along the
72 Brazilian coast started with the migration of Amerindians from the north, arriving in southeastern
73 Brazil about 10,000 years ago (Figuti et al., 2004). Although mostly settled along the coast, these
74 populations also occupied inland forests by around 1800 yr BP (Noelli, 2008). Evidence is strong
75 that Amerindian practices of land use had important impacts on forest structure and composition
76 before the arrival of Europeans (Portes et al., 2018). The first Portuguese settlements were
77 mainly established in Rio de Janeiro state, beginning a period of more intense exploitation of the
78 forest. Today, the southeast is the most populated region of Brazil, but it ironically supports
79 some of the most important remnants of the Atlantic Forest, due to the steep topography and
80 complex relief of montane areas in the region.

81 Most of the large forest remnants in southeastern Brazil are found in protected areas. One of the
82 most important is the Serra dos Órgãos National Park (PARNASO). Located in the northernmost
83 part of the Serra do Mar, PARNASO protects montane rainforest stands and an important
84 complex of UMARF and CDA on a high plateau that supports many rare and endangered species
85 since epiphytes and bamboos till large animals as jaguars (Martinelli and Bandeira, 1989, see
86 also the Brazilian red books for flora and fauna: Martinelli and Moraes, 2013 and ICMBio, 2018).
87 As the climate becomes warmer and wetter, upward migration is expected and the reduction of
88 available habitat for high mountain taxa is a strong possibility (Rull et al., 2009; Vegas-Vilarúbia
89 et al., 2011). Understanding the temporal relationships between climate and vegetation is
90 essential for conservation in the face of climate change, and palaeoecological studies can help to
91 reveal which species and ecosystems may need human intervention to persist (Behling and Pillar,
92 2007; Overbeck et al., 2015; Barnosky et al., 2017). Although the Brazilian highlands have been
93 the object of palaeoecological investigations for more than two decades (e.g., Behling 1995,

94 1997a, 1997b, 2007; Behling et al., 2007; Behling and Safford, 2010; Behling et al., 2020; Ledru
95 et al., 2005; Portes et al., 2018; Raczka et al., 2013; Scheel-Ybert, 2001; Veríssimo et al., 2012),
96 much more remains to be learned about how montane vegetation in this region is influenced by
97 climate, fire and human impacts over the long term.

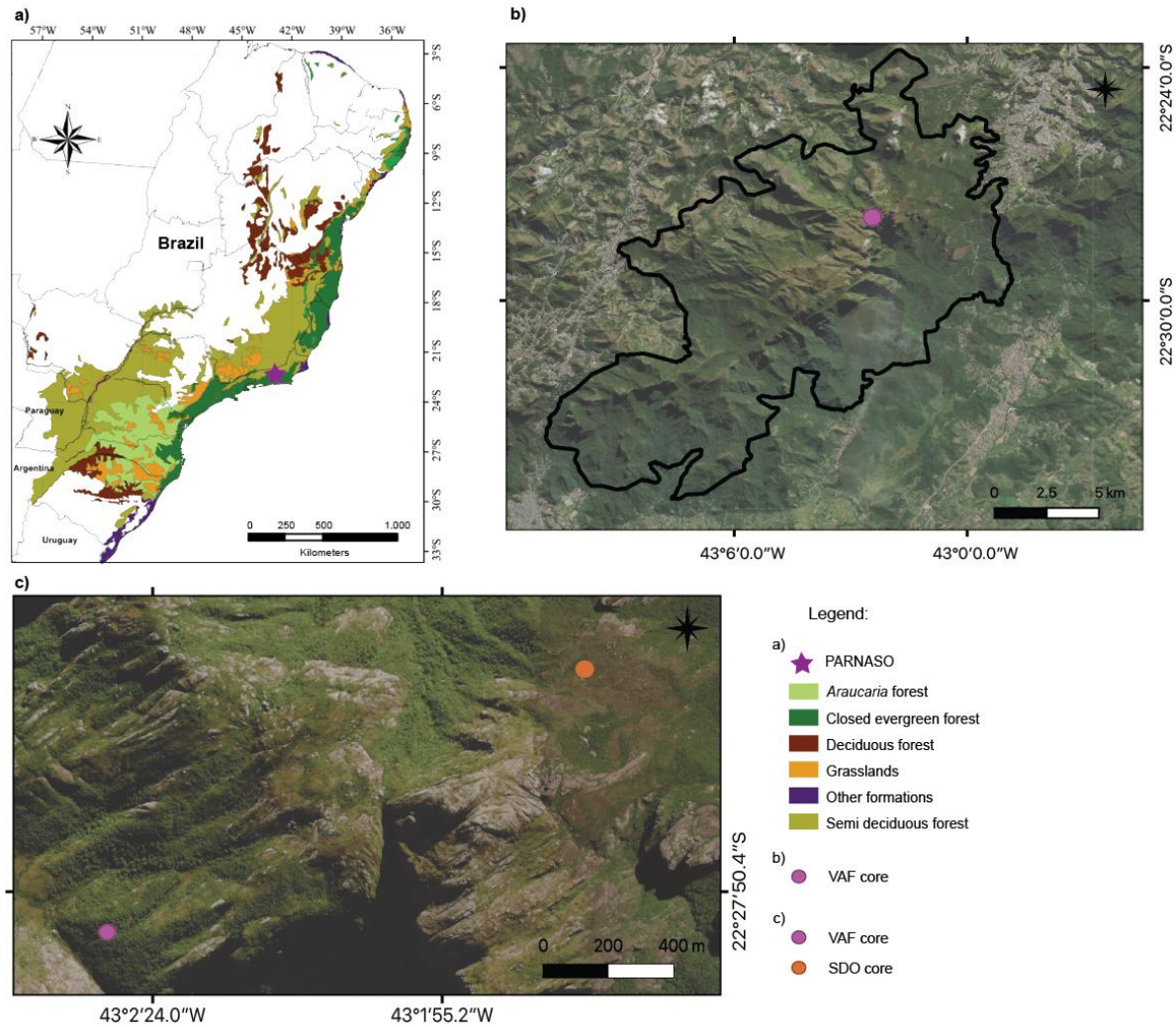
98 Here we report results from a multi-proxy study that analysed temporal vegetation dynamics in a
99 forest patch currently occupied by UMARF and surrounded by CDA vegetation, located near the
100 SDO core sampled by Behling and Safford (2010). Overall, our goal was to better understand
101 temporal dynamics between forest and grassland vegetation in a highly heterogeneous landscape
102 characterized by high biodiversity and high species turnover. Our specific research questions
103 were (1) how did climatic change and fire interact at this montane forest site to influence
104 vegetation composition and dynamics during the Holocene?; and (2) how did Holocene
105 vegetation dynamics differ in this forest patch as compared to the CDA vegetation sampled in
106 the nearby SDO core (Behling and Safford 2010)?

107

108 **ENVIRONMENTAL SETTINGS**

109 The study site is located at 2003 m a.s.l., at latitude 22°27'53.49" S and longitude 43°2'27.04" W
110 in the Serra dos Órgãos National Park (PARNASO), Rio de Janeiro State, southeastern Brazil
111 (Fig. 1). The southeast facing site is characterized by a 2.2 ha patch of upper montane Atlantic
112 Rain Forest (UMARF) bordered by campos de altitude (CDA) in the Serra dos Órgãos, a
113 subrange of the Serra do Mar (Brazilian coastal highlands), about *c.* 90 km from the Atlantic
114 Ocean. Geologic substrate in the study area is Upper Proterozoic granite and granitoid gneiss,
115 uplifted to its present elevation by Cenozoic tectonism associated with widening of the Atlantic
116 Ocean (Riccomini et al., 1989). The Serra dos Órgãos follows a largely NE-SW orientation
117 parallel to the coast. Soils at the study site are generally shallow, poorly developed, acidic and
118 highly organic with high amounts of litter (Falkenberg and Voltolini, 1995).

119



120

121 **Fig. 1.** Location of PARNASO and Vale das Antas Forest (VAF) core. a) national location of
 122 PARNASO (adapted from Fundação SOS Mata Atlântica/ INPE, 2017), b) location of VAF core
 123 in PARNASO and c) distance and vegetation type of VAF core (in UMARF) and SDO core (in
 124 CDA) from Behling and Safford (2010).

125

126 In the region, the climate is mostly controlled by the South Atlantic Convergence Zone (SACZ)
 127 with most precipitation falling between November and April (Safford, 1999a; Vuille et al.,
 128 2012). The climate for the region has been generally defined as mesothermic with mild and wet
 129 summers and moderate winters without a well-defined dry season (Nimer, 1977; ICMBio, 2008).
 130 The nearest long-term meteorological station is found at Teresópolis (22°25.980' S, 42°58.980'
 131 W) at 1100 m a.s.l., where mean annual temperature is 17.6 °C (July mean = 8.6 °C, February

132 mean = 27.2 °C), and mean annual average precipitation is 1800 mm (Hijmans et al., 2005). Our
133 field site is 900 m higher and there is considerable orographic enhancement of precipitation,
134 resulting in a winter without dry season. PARNASO installed temperature data loggers near the
135 study site in September 2012. Between September 17, 2012 and February 2, 2014, the mean
136 overall temperature was 12.7 °C, the maximum was 25.6 °C and the minimum was 1 °C (C.
137 Cronemberger, PARNASO, pers. comm.). Temperatures in the nearby CDA in the Vale das
138 Antas (the study site is in forest slightly above the valley bottom) showed a similar mean
139 temperature (12.5 °C), but temperatures were more extreme due to the lack of trees and the valley
140 bottom position (max = 27 °C, min = -5.2 °C). Safford (unpub. data) also measured winter
141 temperatures in the Vale das Antas campos, in July 1997 a minimum of -9.8 °C was measured,
142 which is the lowest for the Serra dos Órgãos. From regressions against elevation, Safford
143 (1999a,b; Behling and Safford, 2010), estimated precipitation at 2000 m elevation in the Serra
144 dos Órgãos study site to be between 2500 and 3000 mm annually.

145 In the Serra dos Órgãos, CDA vegetation occurs above 1800-2000 m elevation, depending on
146 substrate, topography, slope aspect, and history of disturbance (Safford 1999a). CDA is most
147 common on hilltops and convex slopes, and also dominates poorly-drained valley bottoms
148 (Safford, 1999a; see Fig. 1). Below 1800-2000 m elevation UMARF is the dominant vegetation
149 which gradually replaces tall montane forest above about 1500 m a.s.l., while above these
150 elevations UMRAF becomes more and more restricted to protected sites.

151 The CDA is dominated by graminoids, in PARNASO especially by the giant bunchgrass
152 *Cortaderia modesta*, montane bamboo (*Chusquea pinifolia*), and the large sedge *Machaerina*
153 *ensifolia*. Frequent herb genera include *Eryngium* (Apiaceae) *Paepalanthus*, *Plantago* and *Xyris*
154 (Behling and Safford, 2010). A high number of sclerophyllous shrub taxa is found in the CDA,
155 as well as smaller trees, often in some stage of succession moving toward (after fire or livestock
156 incursion) or away from grassland (long-term lack of disturbance). More open habitats tend to
157 support more woody taxa from Asteraceae (e.g., *Baccharis*, which is a good indicator of campos
158 vegetation). Certain woody taxa from genera such as *Croton* and a number of genera from
159 Myrtaceae (*Myrceugenia*, *Gomidesia*) and Ericaceae (*Gaylussacia*) are also more common in
160 campos habitat. However, most woody taxa in the campos are forest taxa and their density is
161 higher near forest borders. The UMARF is formed by twisted and dwarfed trees and shrubs
162 distributed largely in one stratum normally less than 10 m height. Due to high air humidity and

163 frequent fog there is high abundance and diversity of epiphytes and mosses on tree trunks and
164 branches, rocks and soil (Falkenberg and Voltolini, 1995; Safford, 1999a; Portes et al., 2001).
165 Important tree genera include *Myrsine*, *Weinmannia*, *Clethra*, *Daphnopsis*, *Roupala*, *Symplocos*,
166 *Tibouchina*, *Ilex*, *Ocotea*, and a number of genera from Myrtaceae (Behling and Safford, 2010;
167 Gomes, 2015). Tree ferns of various species are common, as well as epiphytes such as
168 bromeliads and orchids. The grassland-forest ecotone, where scattered trees/open forest cover
169 and understory species co-dominate, is marked by very high habitat heterogeneity. Many
170 herbaceous species from Rubiaceae are especially common in these situations, likewise shrubs of
171 Myrtaceae and Melastomataceae.

172 Our study site consists of an island of UMARF surrounded by CDA vegetation, located in a
173 protected site facing southeast at 2003 m a.s.l. (Fig. 1), around about 1.5 km from the higher
174 located SDO core site at 2130 m a.s.l. (Behling and Safford, 2010).

175

176 **MATERIAL AND METHODS**

177 *Sediment core sampling and dating*

178 In February 2015, a peat deposit was cored an 88 cm-long core was collected in an undisturbed
179 area of UMARF in the Vale das Antas (“Tapir Valley”) and herein called VAF (Vale das Antas
180 Forest). From a base of bedrock, an 88 cm-long core divided in two sections of 50 cm length
181 were extruded onsite using a Russian Corer, wrapped in plastic film and stored under cool (*c.* 4
182 °C) and dark conditions. Six organic bulk sediment samples were collected along the sediment
183 for radiocarbon dating. Two samples were analysed at the Accelerator Mass Spectrometry
184 (AMS) Laboratory at National Taiwan University (NTUAMS) and four samples at the AMS
185 Poznan Radiocarbon Laboratory (LAMS) (Table 2). An HCl test on several core samples was
186 negative and excludes the possibility of a carbon reservoir effect. The age-depth model was
187 performed with R-package Clam 2.2 (Blaauw, 2010) in R-Studio (R-Studio Team, 2016) using
188 the South Hemisphere calibration curve SHCal13.14C and postbomb curve SH 1-2. Calib 7.1
189 was used for calculating the median probability (Stuiver et al., 2019).

190

191 *Palynological analysis*

192 In total 44 subsamples (0.25 cm³) in 2 cm intervals were taken along the core for analysing
193 palynomorphs. Standard pollen techniques were used to process the samples applying 40%

194 hydrofluoric acid (HF) and acetolysis (Faegri and Iversen, 1989). The marker *Lycopodium*
195 *clavatum* (20848±1546, batch 1031) was added to each subsample to determine the pollen
196 concentration (grains cm⁻³) and pollen accumulation rate (grains cm⁻² yr⁻¹) (Stockmarr, 1971).
197 The residue obtained was kept in distilled water and mounted in slides with glycerine for
198 palynomorph analysis under a light microscope. A minimum of 300 pollen grains was counted
199 per sample. Pollen and spores were identified based on the Brazil reference collection of the
200 Department of Palynology and Climate Dynamics at the University of Goettingen, and with
201 support of literature and electronic pollen keys (Behling, 1993; Melhem et al., 2003; Neotropical
202 Fossil Pollen Search Tool developed by Dr. Hermann Behling and Dr. Chengyu Weng
203 [unpublished]). Nomenclature is based on Flora do Brasil 2020 (<http://floradobrasil.jbbr.gov.br>).
204 Pollen and spore percentage were calculated from the pollen sum, including herbs, shrubs, trees,
205 unknowns and excluding ferns, mosses, fungal and Non Pollen Palynomorphs (NPPs). The
206 groups were separated following Behling and Safford (2010) for further comparison: campos de
207 altitude (CDA), upper montane Atlantic Rain Forest (UMARF), other Atlantic Rain Forest
208 (OARF), lowland Atlantic Rain Forest (LARF), ferns (tree ferns and ferns), mosses, fungal
209 spores and NPPs. The pollen diagram was performed with C2 (Juggins, 2007) and portrays the
210 most important taxa based on frequency and dominance. TILIA and TILIAGRAPH were applied
211 to determine pollen assemblage zones based on the stratigraphic constrained cluster analysis of
212 the pollen sum by CONISS (Grimm, 1987).

213

214 ***Macro-charcoal analysis***

215 For analysing the past fire regime and its influence on vegetation, macro-charcoal particles (>150
216 µm) were counted in a total of 176 subsamples of 0.5 cm³ continuously extracted from the core
217 at 0.5 cm resolution. Samples were prepared following the method of Stevenson and Haberle
218 (2005, adapted from Rhodes (1998)) which is a procedure that greatly limits particle
219 fragmentation. 6% H₂O₂ was added to remove organic material in the sediment and samples
220 were gently wet-sieved, retaining particles ≥ 150 µm. Concentrations were determined as
221 particles cm⁻³. Fire regime characteristics were identified using the software CharAnalysis
222 (Higuera, 2009). The data were interpolated to the median temporal resolution (42 years) to
223 obtain the charcoal accumulation rate (CHAR particles cm⁻² yr⁻¹). A window of 1000-year
224 locally weighted regression was applied to separate background (C_{background}) and peak

225 components (C_{peaks}) (Higuera et al., 2010). A Gaussian mixture model was used to identify the
226 C_{noise} distribution. The 99th percentile of the C_{noise} distribution was used to define thresholds.
227 Poisson minimum-count was used to eliminate the peaks from statistically insignificant counts.
228 We used a window of 1000 years to estimate the distribution of fire frequencies. Peak magnitude
229 as an estimate of total charcoal deposition per fire event was used to reflect fuel consumption per
230 fire and/or fire size (Biagioni et al., 2015; Higuera et al., 2010).

231

232 *Loss on ignition*

233 To estimate the organic matter and carbonate content in the sediment, 0.5 cm³ subsamples were
234 continuously extracted from the sediment and immediately weighed. The samples were dried at
235 105 °C for 24 h, dried and combusted at 550 °C during 4 h. Afterward the samples were dried
236 again and OM% was calculated following the method described in Heiri et al. (2001).

237

238 **RESULTS**

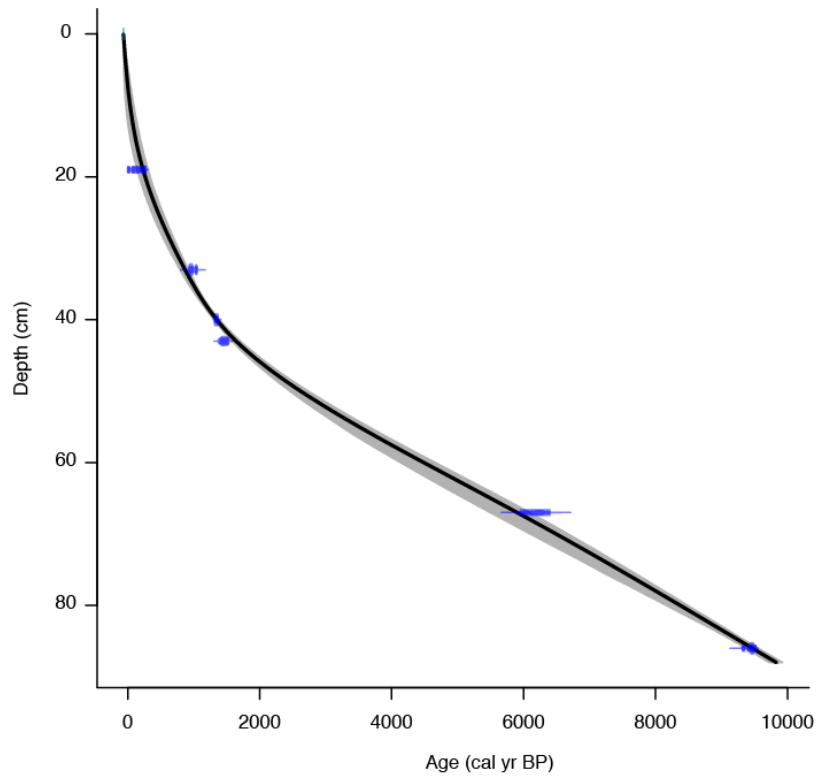
239 *Stratigraphy, chronology and accumulation rate*

240 The 88 cm-long core mostly consists of black organic material on a rocky subsurface. A detailed
241 description is given in Table 1.

242 Six AMS radiocarbon dates were used to construct the age-depth model (Table 2), spanning the
243 period 9840 cal yr BP (calculated age for the lowermost sample at 88 cm) to the present. After
244 testing other age-models, the data were best represented using a 0.3 smoothing spline (Fig. 2).
245 Using this technique, the lowest accumulation rate is at 63 cm (203 yr/cm) while the highest
246 accumulation rate is at present (8 yr/cm). Using interpolation, from the age-depth model the
247 accumulation rate is 170 yr/cm from 88-67 cm core depth, 197 yr/cm from 66-43 cm, 40 yr/cm
248 from 42-40 cm, 52 yr/cm between 39-33 cm, 59 yr/cm from 32-19 cm and 11 yr/cm from 31 to
249 the surface. The median probability was calculated using the software Calib 7.1 (Table 2).

250 Loss-of-ignition analysis demonstrated that the sediment is organic, defined as having more than
251 12% organic carbon. Organic content is lowest in the bottom part of the core, *c.* 30% from 88-60
252 cm depth, while from 60-0 cm depth the average of organic matter is *c.* 38%.

253



254
 255 Fig. 2. Age-depth smoothing spline model for the Vale das Antas core.

256

257 **Table 1.** Stratigraphy of Vale das Antas core.

Depth (cm)	Description
0-20	Black organic material, rather compact and strongly decomposed, some rootless, roots and plant remains
20-41	Black organic material, compact and strongly decomposed, few root fragments
41-61	Black organic material, compact and strongly decomposed, few plant remains, little silty
61-84	Black organic material, compact and completely decomposed, fine sandy
84-88	Black organic material, compact and completely decomposed, few small yellow rocks
88-	Rocky subsurface

258

259

260

261

262

263

264

265

266

267 **Table 2.** AMS radiocarbon dates from VAF core, calibrated age ranges at 95% confidence
 268 intervals.

Lab-code	Depth (cm)	Material dated	Date (¹⁴ C age BP)	Calendar Age (cal yr BP) 2σ	Median probability (cal yr BP)
Poz-106102	19	Organic bulk sediment	180±30	164 – 282 (46.1%) 56 – 123 (25%) -3 – 33 (13.4%) 132 – 157 (10.1%) 39 – 40 (0.3%)	152
Poz-106103	33	Organic bulk sediment	1115±30	927 – 996 (68.5%) 1013 – 1056 (26.4%)	969
Ntuams-2691	40	Organic bulk sediment	1511±9	1315 – 1369 (95%)	1343
Poz-106105	43	Organic bulk sediment	1610±30	1400 – 1531 (90.1%) 1378 – 1393 (4.7%)	1461
Poz-106106	67	Organic bulk sediment	5460±110	5982 – 6406 (92.2%) 5941 – 5974 (2.8%)	6196
Ntuams-2015	86	Organic bulk sediment	8465±44	9396 – 9529 (82.7%) 9308 – 9361 (11.3%) 9375 – 9382 (1%)	9455

269

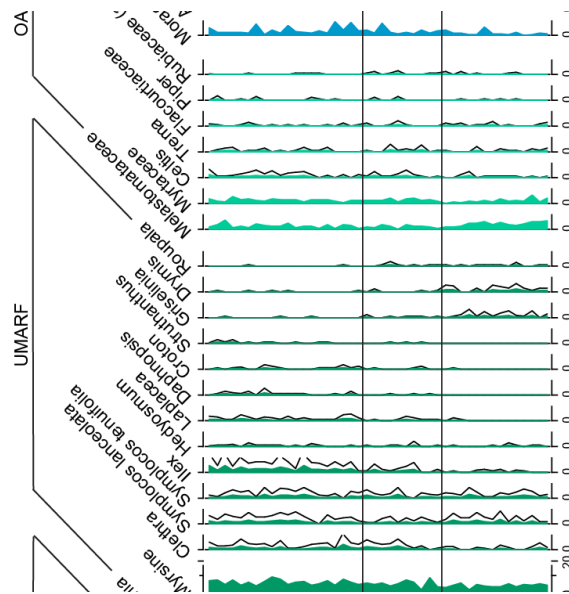
270 *Palynological results*

271 The record is divided into three pollen zones based on the constrained cluster analyses by
 272 CONISS: VAF-I, VAF-II and VAF-III. A total of 94 pollen and 37 spore taxa were identified in
 273 the 44 samples (supplementary material). 12 pollen types remain unidentified. The percentage
 274 pollen diagram (Fig. 3a) shows the dominant and most important taxa grouped into: CDA,
 275 UMARF, OARF, LMARF and ferns. The summary diagram (Fig. 3b) shows the total percentage
 276 sum for each group: CDA, UMARF, OARF, LARF, tree ferns and spores and the sum of all
 277 Asteraceae types. Fig. 3b also includes the depth curves of: sedimentation rate (yr/cm), LOI (%),
 278 charcoal concentration (particles cm⁻³), charcoal accumulation rate (particles cm⁻² yr⁻¹), fire
 279 peaks and fire magnitude.

280

281 VAF-I (88-60 cm; 9840-4480 cal yr BP) – 14 samples

282 This zone is characterized by the dominance of CDA pollen, averaging 61% and ranging from
 283 49% to 69%. Poaceae is the most dominant taxon (46%, > 32% to < 55%), followed by different
 284 Asteraceae types which represent almost 10% of the pollen sum in this zone (> 7.5% to < 12%).
 285 However, *Baccharis* shows its lowest values in the core in this zone (c. 2%). Other taxa
 286 characteristic for the CDA assemblages in VAF-I are Apiaceae (c. 2%), Cyperaceae (1%) and
 287 Fabaceae (1%).



288

289 **Fig. 3a.** Pollen percentage diagram of the most important and most frequent taxa of VAF core
 290 into each group.

291 The average sum of arboreal taxa represents 33% (ranging from 25% to 44%) of the pollen
 292 spectra, and are dominated by UMARF, primarily represented by *Weinmannia* (10%, > 5% to <
 293 17%) and *Myrsine* (6%, > 3% to < 8%). Most taxa of UMARF have their lowest values in this
 294 zone, however *Griselinia* and *Drimys* follow an opposite trend and are found at their highest
 295 densities in this zone, *c.* 1% each. In contrast to the UMARF group, the OARF pollen shows its
 296 highest values in this zone, averaging 8% and ranging from 4% to 13%, with Melastomataceae at
 297 *c.* 4% and Myrtaceae *c.* 2%. LMARF pollen are scarce in VAF-I and only average 3% of the
 298 pollen sum, ranging from 1% to 8%, primarily represented by Moraceae/Urticaceae (1.5%) and
 299 *Alchornea* (1%). Tree ferns occur only as a few single spores. Other fern spores show a roughly
 300 continuously percentage in the zone at about 12% (> 8% to < 17%).

301

302 VAF-II (60-40 cm; 4480-1350 cal yr BP) – 10 samples

303 The pollen CDA percentages slightly decrease to 59%, ranging from *c.* 70% at 50 cm to 54% at
 304 41 cm core depth. Poaceae (43%, > 37% to < 49%) and Asteraceae types (*c.* 12%, > 9% to <
 305 15%) continue as the main taxa, and *Baccharis* increases to *c.* 4%. The arboreal assemblage
 306 reaches *c.* 37% (ranging from 26% to 44%) mostly due to the UMARF group (25%, > 17% to <
 307 31%), characterized mainly by *Weinmannia* (12%, > 8% to < 15%) and *Myrsine* (*c.* 7%, > 3% to
 308 < 11%). *Clethra*, *Symplocos lanceolata*, *S. tenuifolia* and *Ilex* represent *c.* 1% each. The OARF
 309 assemblage gradually decreases to 6.5% (> 3% to < 10%), with Melastomataceae pollen

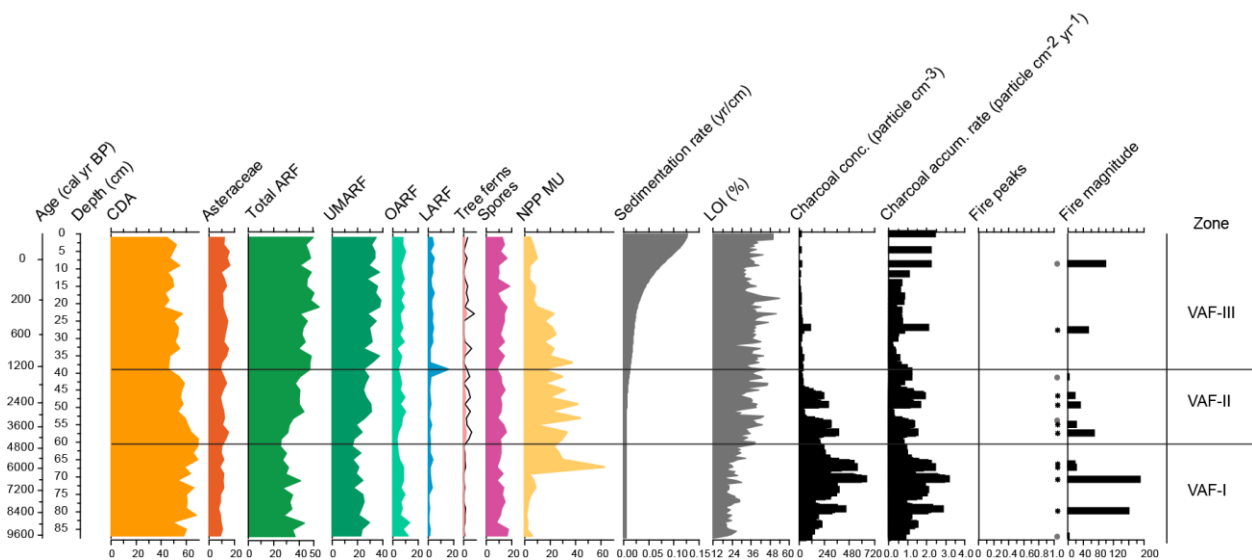
310 declining to less than 2% while Myrtaceae increases to 2.5%. LMARF increases slightly to 4.5%
 311 (> 2% to < 10%) in VAF-II, driven primarily by Moraceae/Urticaceae which reaches almost 3%
 312 (> 15 to < 8.5%). Relatively speaking, tree fern pollen increases greatly in this zone, but only to
 313 c. 1% while other fern spores are stable at 12% (> 9% to < 16%).

314

315 VAF-III (40-0 cm; 1350 cal yr BP to present) – 20 samples

316 In this zone, CDA pollen show a noticeable decrease to 49% (ranging from 42% to 57%) of the
 317 pollen sum. This is primarily driven by the decrease of Poaceae to 32% (> 27% to < 39%).
 318 Asteraceae oscillates but on average maintains the same sum as VAF-II (12%, > 9% to < 16%)
 319 while Cyperaceae reaches its maximum average value of 1.5%. Arboreal pollen increases to
 320 about 47% (ranging from 39% to 56%), led by UMARF pollen at 32% (> 25% to < 38%) and
 321 LMARF pollen at 7.5%. Although *Weinmannia* and *Myrsine* remain the most important taxa in
 322 the UMARF group, increasing to 15% (> 11% to < 22%) and c. 8% (> 6% to < 12%)
 323 respectively, other taxa also contribute to the increase in VAF-III. *Clethra*, *S. lanceolata*, *S.*
 324 *tenuifolia* occur with c. 1% each and *Ilex* reaches about 2%. OARF continues with c. 7%
 325 (ranging from 3% to 10%), and its main taxa (Melastomataceae and Myrtaceae) remain constant.
 326 A stronger change is observed in LMARF, which reaches its maximum (mean = 7.5%, varying
 327 from 3% to 20%), due to the expansion of Moraceae/Urticaceae (3.7%), *Alchornea* (2%),
 328 *Cecropia* (1%) and *Euterpe/Geonoma* (0.7%). As in the previously zones, non-tree fern spores
 329 are at 12% (> 8.5% to < 16%), while tree ferns show slightly reduced values.

330



331 **Fig. 3b.** Summary diagram of the Vale das Antas Forest core, showing the ecological groups
332 (%), sedimentation rate (yr/cm), loss of ignition (%), macro-charcoal concentration (particle cm⁻³)
333 and accumulation rate (particle cm⁻²yr⁻¹), fire peaks and fire magnitude. A 5x exaggeration
334 scale line is shown for low percentage values

335

336 *Macro-charcoal and fire regime*

337 The CharAnalysis of macro-charcoal characterize the fire history for the past 9840 years (Fig.
338 3b). Average concentration for the entire sediment is 190 particles cm⁻³, decreasing from 250
339 particles cm⁻³ in zone VAF-I, to 150 particles cm⁻³ in VAF-II and only 30 particles cm⁻³ in zone
340 VAF-III. The local signal-to-noise exceeds 3.5, indicating a good separation between peak and
341 non-peak values. From 13 fire peaks, 4 fire episodes failed to pass the Poisson minimum-count
342 criterion, including the most recent peak at 9 cm depth (19 cal yr BP). The most recent
343 significant peak is found at 28 cm depth, (565 cal yr BP). The mean fire return interval (FRI,
344 95% probability) calculated with a 1000-yr window and only using fires that met the minimum-
345 count criterion is 998 yr (593-1449 yr). Using all 13 identified fire peaks and calculating the FRI
346 across the entire record yields an FRI of 617 (446-827 yr). Under either measure, local fire
347 events (fires within 500 m or so of the core site) were rare over the period of our sample, but the
348 nearly continuous presence of charcoal through the core demonstrates fires were not regionally
349 uncommon. Most fire peaks as well as the highest magnitude peaks occurred in zone VAF-I.

350

351 **INTERPRETATION AND DISCUSSION**

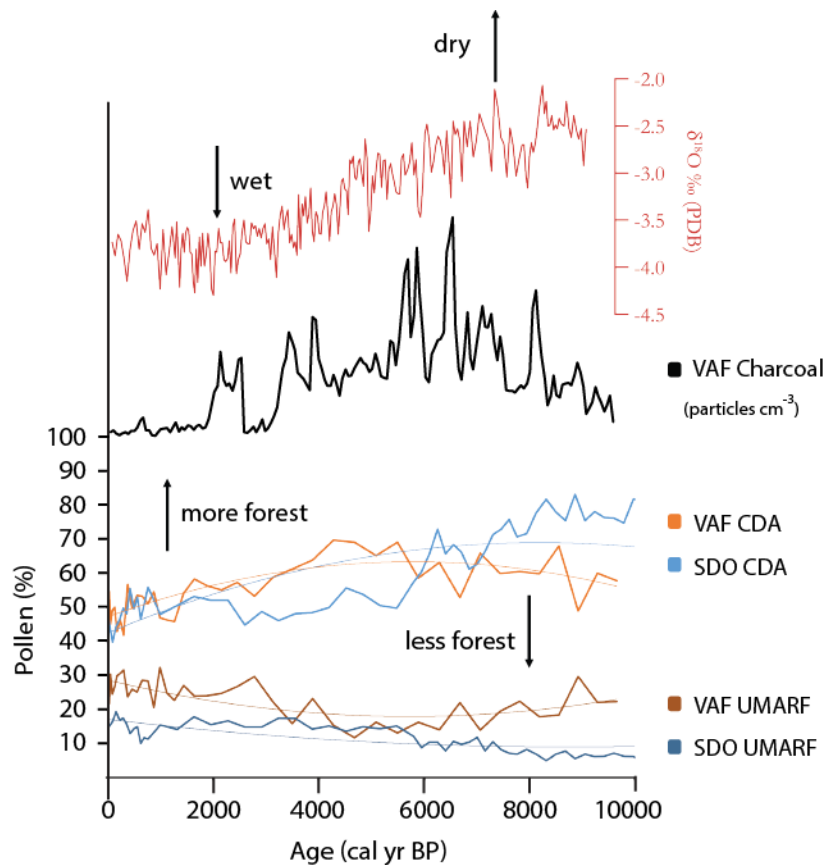
352 Overall, the stratigraphy and the organic content of the VAF core in the Serra dos Órgãos
353 National Park indicate that there was a change from drier to wetter climatic conditions in the
354 region during the Holocene, demonstrated by the lower accumulation rate and lower organic
355 matter in the bottom part of the core. From the beginning of the pollen record, the general study
356 area was dominated by CDA, rich in grass and shrubs, mostly represented by species of Poaceae,
357 Asteraceae, Apiaceae and Cyperaceae. Forest cover at high elevations (>1800 m) in the Serra dos
358 Órgãos and other mountains in southeastern Brazil is extremely heterogeneous and controlled
359 largely by climo-topographic and soils variables in combination with disturbance (Safford,
360 1999a,b; 2001). Other studies of palaeovegetation in the southeastern Brazilian mountains
361 (Behling, 1997b; Behling et al. 2007; Behling and Safford, 2010; Veríssimo et al., 2012; Behling

362 et al., 2020) show a trend of increasing forest cover – and decreasing campos cover – at high
363 elevations since the Early Holocene, with acceleration in this trend during the Late Holocene,
364 indicating that climates during the Early Holocene were much drier than today and CDA
365 vegetation was much more widespread than today.

366 Our pollen data suggest that UMARF was not widely distributed at higher elevations (>1800 m)
367 in the Serra dos Órgãos in Zone I (9840-4480 cal yr BP), and that the more continuous local
368 forest may not have developed until after 1350 cal yr BP (Zone III). Before 4480 cal yr BP the
369 study site was rich in genera of southern temperate-latitude ancestry such as *Weinmannia*,
370 *Drimys* and *Griselinia*, implying a somewhat colder climate than today. UMARF taxa of tropical
371 origin were also represented in the Early Holocene pollen, but their abundances were mostly low
372 or very low before they began to rise substantially after 4480 yr cal BP. Examples of this pattern
373 include *Clethra*, *Ilex*, *Laplacea*, *Daphnopsis*, *Croton*, and the tree ferns. Some UMARF genera
374 were already relatively common before 4480 cal yr BP but saw their abundances rise further
375 thereafter. Examples are *Weinmannia* (2x increase) and *Myrsine* (50% increase). *Symplocos*,
376 Melastomataceae and Myrtaceae (the latter two very common in both UMARF and OARF)
377 showed similar abundances throughout the Holocene. The modern UMARF is characterized by
378 species of temperate, neotropical and tropical origin which occur in the majority of UMARF in
379 southeastern and southern Brazil (e.g. Portes et al., 2001; Safford, 2007; Scheer and
380 Mocoichinski, 2009; Gomes, 2015; Moreira et al., 2018).

381 Modern pollen rain data from the Serra dos Órgãos (Portes et al., 2020) suggest that current areas
382 of CDA are under-represented in pollen assemblage due to the low pollen production and low
383 accumulation rate of CDA taxa and also the over-representation of some arboreal taxa, especially
384 pioneer or secondary species of montane forest upwards wind-transported. They propose the use
385 of a restricted group of typical upper montane forest, which should be more sensitive to detect
386 the local trend of forest changes (within the mosaic landscape) than the full groups of ARF.
387 Therefore, following Portes et al. (2020), we aggregated pollen sums from *Weinmannia*,
388 *Myrsine*, Myrtaceae and *Clethra* to represent UMARF and aggregated the same taxa used by
389 Behling and Safford (2010) to represent the CDA. Fig. 4 shows the temporal trends in forest and
390 in CDA from our VAF core and the SDO core sampled by Behling and Safford (2010) (which
391 stretched back into the Late Pleistocene [12380 cal yr BP]), and superimposes the macro-
392 charcoal concentration (particles cm⁻³) from VAF core and the $\delta^{18}\text{O}$ record from Bernal et al.

393 (2016). Our data suggest that the study site was dominated by CDA vegetation for most of the
 394 Holocene, with more or less uniform CDA vegetation in the Early Holocene and a notable
 395 contraction in the Late Holocene after about 4500 yr BP, corroborating the higher charcoal
 396 concentration as well as the drier climate at that period. As climate became wetter after around
 397 1400 cal yr BP, charcoal concentration decreases, the CDA:forest ratio drops to 50:50 and the
 398 group of upper montane ARF increases to around 30%. The SDO core shows similar patterns,
 399 with an accentuated increase in forest pollen after about 5000 cal yr BP, and the balance of
 400 campos vs. forest pollen dropping below 50:50 after around 1500 cal yr BP (Fig. 4). While VAF
 401 core was collected in a currently UMARF patch surrounded by CDA vegetation, SDO core was
 402 cored from a more widespread CDA vegetation. We hypothesize therefore that the patch of
 403 forest that currently occupies the VAF site has only been extant since sometime in the Late
 404 Holocene, although the pollen data make clear that upper montane forest taxa have been in the
 405 broader region throughout the Holocene.



406
 407 **Fig. 4.** Comparison of the sum (%) of *Weinmannia*, *Myrsine*, Myrtaceae and *Clethra* taxa
 408 representing UMARF from VAF core (VAF UMARF), the sum of *Weinmannia*, *Myrsine*,

409 Myrtaceae and *Clethra* taxa representing UMARF from SDO core (SDO UMARF), the sum of
410 CDA group from VAF core (VAF CDA) and the sum of CDA group from SDO core (SDO
411 CDA), plotted with macro-charcoal concentration (particles cm⁻³) from VAF core and $\delta^{18}\text{O}$
412 record from Botuverá Cave (Bernal et al., 2016) for the last 10,000 years. Trendline from 2nd
413 order polynomial.

414

415 The VAF core also documents temporal floristic variation that points to important changes in
416 climate over the course of the Holocene. We interpret the Early and Mid-Holocene as relatively
417 cool and dry (but becoming gradually warmer and wetter over time), based on (1) the general
418 lack of tree ferns; (2) low LOI values; (3) relatively high frequencies and magnitudes of fire; (4)
419 relatively low pollen densities for *Baccharis*, which is a faithful campos indicator but under
420 warmer temperatures; and (5) the elevated presence of cool climate indicators of southern
421 temperate ancestry like *Drimys* and *Griselinia*. In addition, the nearby SDO core records
422 *Araucaria* pollen until about 10,800 cal yr BP, further pointing to cooler Early Holocene
423 temperatures. UMARF vegetation in the Early and Mid-Holocene seems to have been somewhat
424 composed of a more southern-temperate flora.

425 Zones VAF-II (4480-1350 cal yr BP) and III (1350 cal yr BP to present) represent the Late
426 Holocene. After 4480 cal yr BP organic matter in the soil increased in coincidence with increases
427 in a number of UMARF and OARF taxa. Taxa of tropical origin such as *Clethra*, *Symplocos*,
428 *Celtis*, *Trema* and Flacourtiaceae expanded, as did the tree ferns. Associated with the rising
429 elevation and expanse of forest, fire magnitude and frequency declined suggesting a shift to
430 wetter conditions. A shift to even wetter conditions appears to have occurred at the beginning of
431 VAF-III (around 1350 cal yr BP), demonstrated by a strong and abrupt intensification of
432 sediment accumulation, a decrease in charcoal concentration, and a reduction of CDA pollen to
433 *c.* 50% of the total. The sharp peak of *Alchornea* just after 1350 cal yr BP and the increase in
434 other tropical LARF taxa (Moraceae/Urticaceae, *Cecropia* and *Euterpe/Geonoma* type) are
435 indicative of a rapid change toward a warmer and wetter climate in the Late Holocene. Since
436 about 1200 cal yr BP the CDA/UMARF relationship has remained in an approximate balance in
437 the study area. During this period, the last significant fire peak at *c.* 600 cal yr BP occurred and
438 may be related to the VAF-III peak in CDA pollen and concurrent drop in UMARF pollen that
439 occurs shortly thereafter.

440 Other studies also suggest an intensification in Late Holocene precipitation. Moss spores in the
441 nearby SDO core increased greatly in the Late Holocene sediment (Behling and Safford, 2010).
442 Palaeoclimate data from the last 10,000 years at Botuverá Cave (27°13'S, 49°09'W, 230 m a.s.l.;
443 Bernal et al., 2016) registered an increase in rainfall starting about 4000 years ago (see Fig. 4)
444 which coincides with the spread of forest vegetation and declining occurrence and magnitude of
445 fire in our core. Evidence for a relatively sudden increase in precipitation in VAF (see above) at
446 around 1350 cal yr BP is also supported by studies of the SAMS (South American Monsoon
447 System) over the last 2000 years, which show a strengthening monsoon during the Little Ice Age
448 (LIA), resulting in a wetter period from *c.* 1400-1800 AD (Vuille et al., 2012).
449 Charcoal in the VAF and SDO cores suggests that fires have occurred in the Serra dos Órgãos
450 since at least the Late Pleistocene, i.e., before the documented arrival of humans in southeastern
451 Brazil, which probably arrived in the region around 10,000 years ago (Figuti et al., 2004).
452 Longer records from other CDA sites in the southeastern Brazilian mountains show notably more
453 fire even further back in time, such as the 35,000 years record from Morro do Itapeva in the
454 southern Serra da Mantiqueira (Behling, 1997b), and the 18,600 years record from the Serra da
455 Bocaina (Behling et al., 2007). However, fires in the immediate locality of the VAF core were
456 infrequent during the Holocene. By using relatively large macro-charcoal (>150 µm) in our
457 CharAnalysis, we restricted our assessment to fires that occurred within probably 500 m or so of
458 the core site (Higuera et al., 2007). This permits a more site-specific understanding of fire history
459 and suggests that the Holocene fire return interval in this wet but seasonally dry landscape was
460 long, ranging from around 600 to 1000 years (depending on our assumptions). It is also clear
461 however that fires were, and usually still are, relatively small, and our analysis thus under-
462 represents the fire regime of the broader landscape. The Serra dos Órgãos landscape is
463 topographically extremely abrupt and heterogeneous (the rise from Guapimirim to Pedra do Sino
464 is 2210 m in less than 8 km and some of the tallest rock walls in all of Brazil are found here), and
465 the high mountain summits and plateau that support CDA are small, ringed by cliffs and humid
466 forest, and cut by deep gorges (see Fig. 1). As a result, lightning ignitions that occur on
467 topographic eminences with combustible fuels (graminoids or dry woody fuels) have little
468 chance to spread far. Most lightning strikes in southeastern Brazil occur during the wet season,
469 but lightning at either the beginning or end of the wet season has the potential to cause fire
470 (Safford, 2001). Today most ignitions are anthropogenic and occur during the dry season, when

471 lightning ignitions are far more rare. Human ignitions that occur during very warm and
472 especially windy conditions can spread from mountain to mountain and even burn appreciable
473 areas of forest. Control of such fires is a major conservation issue in the Brazilian National Park
474 system.

475 Another reason our charcoal analyses almost certainly under-represent palaeofire frequencies in
476 the CDA is that macro-charcoal (>150 μm) is composed of charred woody fragments, but
477 graminoids are the principal fuel for fire in the campos. Whitlock et al. (2004) note that the best
478 correspondence between real fire frequency and charcoal records is where woody vegetation is
479 dense and continuous, a condition that is rare at the highest elevations of the Serra do Mar.
480 Behling et al. (2020) found a similar site-specific fire return interval for the AN core from the
481 Serra do Itatiaia (mean = 630 years through the Mid- and Late Holocene) and noted similar
482 issues with the dominance of graminoid vegetation in the surrounding landscape. Obvious
483 directions for further research are to (1) conduct macro-charcoal analysis on already published
484 cores that predated the development of the analytical techniques (such cores exist from a number
485 of high montane sites in southeast Brazil); (2) obtain sediment core samples from more – and
486 both elevationally and vegetationally more varied – locations in the southeastern Brazilian
487 highlands; and (3) develop new techniques to better assess fire frequencies and magnitudes using
488 charcoal from herbaceous sources.

489

490 **SUMMARY AND CONCLUSION**

491 Like other studies of palaeovegetation in the southeastern Brazilian mountains (i.e. Behling and
492 Safford, 2010; Behling et al., 2007; Scheel-Ybert, 2001; Veríssimo et al. 2012), the VAF record
493 shows a clear trend from drier to wetter climatic conditions during the Holocene, and a clear
494 trend of replacement of CDA vegetation by forest vegetation. The results indicate that the higher
495 elevations of Serra dos Órgãos have been occupied by a mosaic of CDA and UMARF since the
496 beginning of the record (9840 cal yr BP) although the forest patch that occupies the VAF site has
497 probably been extant only since about 1350 cal yr BP.

498 Both the VAF record (collected in a forest patch) and SDO record (cored in CDA vegetation)
499 indicate that CDA was much more widespread in the Late Holocene than it is today and both
500 core sites also demonstrate a similar pattern of forest moving consistently upwards through much
501 of the Holocene. This is especially the case for UMARF taxa but also for montane ARF. At

502 around 1000 cal yr BP (1350 cal yr BP in VAF and 880 cal yr BP in SDO) the data indicate a
503 marked shift toward a warmer and wetter climate, further favouring the expansion of forest
504 vegetation. The variability in timing of these climatic events between the two cores are likely
505 related to differences in vegetation and relief as well as the error intrinsic to ^{14}C dating.
506 The macro-charcoal record in the VAF core corroborates changes seen in climate and vegetation.
507 Fires were more frequent and of greater magnitude in the Early Holocene, decreased after around
508 4000 cal yr BP, and have been very rare in the Late Holocene. The nearby SDO core (Behling
509 and Safford 2010) showed similar patterns, with more frequent fire during the Early Holocene,
510 especially from 10,800 to 7850 cal yr BP, and a decreasing trend until about 5640 cal yr BP,
511 when charcoal concentrations and accumulation more or less levelled off.
512 Our results support the conclusions of previous studies (e.g., Behling, 1997b; Safford, 2001;
513 Behling et al., 2007; Behling and Safford, 2010; Veríssimo et al., 2012) that fire has long been a
514 natural disturbance factor in the campos de altitude. Nevertheless, before the arrival of humans at
515 these mountain sites, fires mostly occurred during the wet season and today anthropogenic
516 ignitions occur primarily during the dry season in very warm and windy conditions and fire sizes
517 can be enormous. Further research is needed to better define the natural fire regime in the
518 Brazilian Highlands. Another conservation concern is the long-term increase in precipitation and
519 temperature that has been underway for centuries and is rapidly accelerating as greenhouse gas
520 emissions rise. Forest expansion into previously grassland-dominated sites threatens the habitat
521 heterogeneity than underlies the high biodiversity and endemism of these montane sites (Safford,
522 2001; Portes et al., 2018). We recommend that protected areas containing campos de altitude and
523 upper montane rain forest develop management strategies that incorporate observation,
524 measurement, experimentation, and active management techniques that help to retain landscape
525 heterogeneity (see Portes et al., 2018). The standard “hands-off” protectionism that has
526 characterized national park management for the last century may be particularly poorly suited to
527 conservation in an age of rapid global change (Cole and Yung, 2010; Safford et al., 2012).

528

529 **ACKNOWLEDGEMENTS**

530 We are very thankful to the ICMBio – Instituto Chico Mendes de Conservação da
531 Biodiversidade, original institution of the first author and for given permission to develop this
532 research in the PARNASO. We also thank Cecilia Cronemberger from PARNASO and José

533 Guilherme Carvalho da Costa for helping in the fieldwork. We thank Dr. Vera Markgraf and one
534 anonymous reviewer for their important reviews. This work was supported by the Ciências sem
535 Fronteiras/CNPq program, Brazil (grant nº 232876/2014-2) given to the first author.

536

537 **REFERENCES**

538 Barnosky, A.D., Hadly, E.A., Gonzalez, P., Head, J., Polly., P.D., Lawing, A.M. et al., 2017.
539 Merging paleobiology with conservation biology to guide the future of terrestrial
540 ecosystems. *Science* 355, issue 6325 DOI: 10.1126/science.aah4787.

541 Behling, H., 1993. Untersuchungen zur Spätpleistozänen und Holozänen Vegetations- und
542 Klimageschichte der Tropischen Küstenwälder und der Araukarienwälder in Santa Catarina
543 (Südbrasilien). (PhD thesis). J. Cramer, Berlin, Stuttgart.

544 Behling, H., 1995. Investigations into the Late Pleistocene and Holocene history of the
545 vegetation and climate in Santa Catarina (S Brazil). *Vegetation History and Archaeobotany*
546 4, 127-152.

547 Behling, H., 1997a. Late Quaternary vegetation, climate and fire history of the Araucaria forest
548 and campos region from Serra Campos Gerais, Paraná State (South Brazil). *Review of*
549 *Palaeobotany and Palynology* 97, 109-121.

550 Behling, H., 1997b. Late Quaternary vegetation, climate and fire history from the tropical
551 mountain region of Morro de Itapeva, SE Brazil. *Palaeo* 129, 407-422.

552 Behling, H., 2007. Late Quaternary vegetation, fire and climate dynamics of Serra do Araçatuba
553 in the Atlantic coastal mountains of Paraná State, southern Brazil. *Vegetation History and*
554 *Archaeobotany* 16, 77-85.

555 Behling, H., Pillar, V.D., 2007. Late Quaternary vegetation, biodiversity and fire dynamics on
556 the southern Brazilian highland and their implication for conservation and management of
557 modern Araucaria forest and grassland ecosystems. *Phil. Trans. R. Soc. B* 362, 243-251.

558 Behling, H., Safford, H.D., 2010. Late-glacial and Holocene vegetation, climate and fire
559 dynamics in the Serra dos Órgãos, Rio de Janeiro State, southeastern Brazil. *Global Change*
560 *Biology* 16, 1661-1671.

561 Behling, H., Dupont, L., Safford, H.D., Wefer, G., 2007. Late Quaternary vegetation and climate
562 dynamics in the Serra da Bocaina, southeastern Brazil. *Quaternary International* 161, 22-31.

563 Behling, H., Jantz, N., Safford, H.D., 2020. Mid- and late Holocene vegetation, climate and fire

564 dynamics in the Serra do Itatiaia, Rio de Janeiro State, southeastern Brazil. *Review of*
565 *Palaeobotany and Palynology* 274, 104-152.

566 Bernal, J.P., Cruz, F.W., Stríkis, N.M., Wang, X., Deininger, M., Catunda, M.C.A., Ortega-
567 Obregón, C., Cheng, H., Edwards, R.L., Auler, A.S., 2016. High-resolution Holocene South
568 American monsoon history recorded by a speleothem from Botuverá Cave, Brazil. *Earth*
569 *and Planetary Science Letters* 450, 186-196.

570 Biagioni, S., Krashevskaya, V., Achnoph, Y., Saad, A., Sabiham, S., Behling, H., 2015. 8000
571 years of vegetation dynamics and environmental changes of a unique inland peat ecosystem
572 of the Jambi Province in Central Sumatra, Indonesia. *Palaeogeography, Palaeoclimatology,*
573 *Palaeoecology* 440, 813-829.

574 Blaauw, M., 2010. Methods and code for ‘classical’ age-modelling of radiocarbon sequences.
575 *Quaternary Geochronology* 5, 512–18.

576 Câmara, I.G., 2003. Brief history of conservation in the Atlantic Forest. In: Galindo- Leal, C.,
577 Câmara, I.G. (Eds.), *The Atlantic Forest of South America: Biodiversity Status, Threats, and*
578 *Outlook*. CABS and Island Press, Washington, pp. 31–42.

579 Cole, D.N., Yung, L., eds., 2010. *Beyond naturalness: Rethinking park and wilderness*
580 *stewardship in an era of rapid change*. Island Press, Washington, DC, USA.

581 Dean, W., 1995. *With Broadax and Firebrand: The destruction of the Brazilian Atlantic Forest*.
582 University of California Press, Berkeley.

583 Faegri, K., Iversen, J., 1989. *Textbook of modern pollen analysis*. 4th ed. John Wiley and Sons,
584 Chichester.

585 Falkenberg, D. B., Voltolini, J. C., 1995. The Montane Cloud Forest in Southern Brazil. In:
586 Hamilton, L. S., Juvik, J. O., Scatena, F. N. (eds.) *Tropical Montane Cloud Forests*.
587 *Ecological Studies* 110, New York: Springer-Verlag, p. 138-149.

588 Figuti, L., Eggers, S., Mendonça, C.A., Porsani, J.L., Rocha, E.B., De Blasis, P.A.D., Bissa,
589 W.M., 2004. *Investigações arqueológicas e geofísicas dos sambaquis fluviais do vale do*
590 *Ribeira de Iguape, Estado de São Paulo*. Museu de Arqueologia e Etnologia, USP. Relatório
591 Final de Atividades de Projeto Temático, processo FAPESP n° 1999/12684-2, período:
592 6/2003 a 4/2004.

593 Flora do Brasil, 2020. Jardim Botânico do Rio de Janeiro. Available at:
594 <http://floradobrasil.jbrj.gov.br/>

595 Fundação SOS Mata Atlântica/ INPE - Instituto Nacional de Pesquisas Espaciais, 2017. Atlas
596 dos remanescentes florestais da Mata Atlântica - período 2015 - 2016. Relatório técnico.
597 São Paulo.

598 Gomes, C. G., 2015. Composição florística e estrutural do componente arbóreo de um fragmento
599 de mata nebulosa no Parque Nacional da Serra dos Órgãos, Rio de Janeiro, Brasil. Graduate
600 dissertation, unpublished.

601 Grimm, E. C., 1987. CONISS: a FORTRAN 77 program for stratigraphically constrained cluster
602 analysis by the method of incremental sum of squares. *Computers and Geosciences* 13, 13–
603 35.

604 Heiri, O., Lotter, A.F., Lemcke, G., 2001. Loss on ignition as a method for estimating organic
605 and carbonate content in sediments: reproducibility and comparability of results. *Journal of*
606 *Paleolimnology* 25, 101-110.

607 Higuera, P., 2009. CharAnalysis 0.9: diagnostic and analytical tools for sediment-charcoal
608 analysis. User's guide. Montana State University. <http://CharAnalysis.googlepages.com>.

609 Higuera, P.E., Peters, M.E., Brubaker, L.B., Gavin, D.G., 2007. Understanding the origin and
610 analysis of sediment-charcoal records with a simulation model. *Quaternary Science*
611 *Reviews* 26, 1790-1809.

612 Higuera, P.E., Gavin, D.G., Bartlein, P.J., Hallet, D.J., 2010. Peak detection in sediment-charcoal
613 records: impacts of alternative data analysis methods on fire-history interpretations.
614 *International Journal of Wildland Fire* 19, 996-1014.

615 Hijmans, R.J., Cameron, S.E., Parra, J.L., Jones, P.G., Jarvis, A., 2005. Very high resolution
616 interpolated climate surfaces for global land areas. *International Journal of Climatology* 25,
617 1965-1978. WorldClim – Global Climate Data, extracted in 8/05/2019.

618 Hueck, K., 1966. Die Wälder Südamerikas. Ökologie, Zusammensetzung und wirtschaftliche
619 Bedeutung. Gustav Fischer Verlag, Stuttgart.

620 ICMBio – Instituto Chico Mendes de Conservação da Biodiversidade, 2008. Plano de Manejo do
621 Parque Nacional da Serra dos Órgãos. Available at
622 [http://www.icmbio.gov.br/portal/component/content/article?id=2196:parna-da-serra-dos-
623 orgaos](http://www.icmbio.gov.br/portal/component/content/article?id=2196:parna-da-serra-dos-
623 orgaos).

624 ICMBio – Instituto Chico Mendes de Conservação da Biodiversidade, 2018. Livro vermelho da
625 fauna brasileira ameaçada de extinção, vol. I. 1 ed. ICMBio/MMA, Brasília, DF. 492 p.

626 (available at <https://www.icmbio.gov.br/portal/component/content/article/10187>).

627 Juggins, S., 2007. C2 User Guide: Software for Ecological and Palaeoecological Data Analysis
628 and Visualization. University of Newcastle, Newcastle upon Tyne, UK, 1–73.

629 Ledru, M.P., Rousseau, D.D., Cruz Jr., F.W., Riccomini, C., Karmann, I., Martin, L., 2005.
630 Paleoclimate changes during the last 100,000 yr from a record in the Brazilian Atlantic
631 rainforest region and interhemispheric comparison. *Quaternary research* 64, 444-450.

632 Ledru, M.P., Mourguiart, P., Riccomini, C., 2009. Related changes in biodiversity, insolation and
633 climate in the Atlantic rainforest since the last interglacial. *Palaeogeography, Palaeoclimatology, Palaeoecology* 271, 140-152.

634

635 Martinelli, G., Bandeira, J., 1989. Campos de altitude. Editora Index, Rio de Janeiro.

636 Martinelli, G., Moraes, M.A. 2013. Livro vermelho da flora do Brasil. 1. ed. Instituto de
637 Pesquisas Jardim Botânico do Rio de Janeiro. Rio de Janeiro. 1100 p. (available at
638 https://dados.gov.br/dataset/portaria_443).

639 Melhem, T.S., Cruz-Barros, M.A.V, Côrrea, A.M.S., Makino-Watanabe, H., Silvestre-Capellato,
640 M.S.F., Esteves, V.L.G., 2003. Variabilidade Polínica em Plantas de Campos do Jordão
641 (São Paulo, Brasil). *Boletim do Instituto de Botânica de São Paulo*, São Paulo.

642 Moreira, B., Carvalho, F.A., Menini Neto, L., Salimena, F.R.G., 2018. Phanerogamic flora and
643 phytogeography of the Cloud Dwarf Forests of Ibitipoca State Park, Minas Gerais, Brazil.
644 *Biota Neotropica* 18(2).

645 Myers, N., Mittermeier, R. A., Mittermeier, C. G., Fonseca, G. A. B., Kent, J., 2000.
646 Biodiversity hotspots for conservation priorities. *Nature* 403, 853-858.

647 Nimer, E., 1977. Clima. In: IBGE - Instituto Brasileiro de Geografia e Estatística. geografia do
648 Brasil: região sudeste, vol. 3. SERGRAF - IBGE, Rio de Janeiro, pp. 51-90.

649 Noelli, F.S., 2008. The Tupi expansion. In: H Silverman and W.H. Isbell (Eds), *Handbook of*
650 *South American Archaeology*, Springer, New York, Chapter 33, pp. 659-670.

651 Oksanen, J., Blanchet, F. G., Friendly, M., Kindt, R., Legendre, P., McGlenn, D., Minchin, P. R.,
652 O'Hara, R. B., Simpson, G. L., Solymos, P., Stevens, M. H. H., Szoecs, E., Wagner, H.,
653 2019. *Vegan: Community Ecology Package*. R package version 2.5-5. [https://CRAN.R-](https://CRAN.R-project.org/package=vegan)
654 [project.org/package=vegan](https://CRAN.R-project.org/package=vegan).

655 Overbeck, G.E., Vélez-Martin, E., Scarano, F.R., Lewinsohn, T.M., Fonseca, C.R., Meyer, S.T.,
656 Müller, S.C., Ceotto, P., Dadalt, L., Durigan, G., Ganade, G., 2015. Conservation in Brazil

657 needs to include non-forest ecosystems. *Diversity and Distributions* 21(12), 1455-1460.

658 Portes, M.C.G.O., Galvão, F., Koehler, A., 2001. Caracterização florística e estrutural de uma
659 Floresta Ombrófila Densa Altomontana do morro Anhangava, Quatro Barras, PR. *Revista*
660 *Floresta* 31(1/ 2), 22-31.

661 Portes, M.C.G.O., Safford, H., Behling, H., 2018. Humans and climate as designers of the
662 landscape in Serra da Bocaina National Park, southeastern Brazil, over the last seven
663 centuries. *Anthropocene* 24, 61-71.

664 Portes, M.C.G.O., Safford, H., Montade, V., Behling, H., 2020. Pollen rain-vegetation
665 relationship along an elevational gradient in the Serra dos Órgãos National Park,
666 southeastern Brazil. *Review of Palaeobotany and Palynology* 283,
667 <https://doi.org/10.1016/j.revpalbo.2020.104314>.

668 Prentice, I.C., 1980, Multidimensional scaling as a research tool in Quaternary Palynology: a
669 review of theory and methods. *Review of Palaeobotany and Palynology* 31, 71-104.

670 Raczka, M.F., de Oliveira, P.E., Bush, M., McMichael, C.H., 2013. Two paleoecological
671 histories spanning the period of human settlement in southeastern Brazil. *Journal of*
672 *Quaternary Science* 28, 144-151.

673 Ribeiro, M.C., Metzger, J.P., Martensen, A. C., Ponzoni, F.J., Hirota, M, M., 2009. The Brazilian
674 Atlantic Forest: How much is left, and how is the remaining forest distributed? Implications
675 for conservation. *Biological Conservation* 142, 1141-1153.

676 Riccomini, C., Peloggia, A.U., Saloni, J.C.L., Kohnke, M.W., Figueira, R. M., 1989. Neotectonic
677 activity in the Serra do Mar rift system (southeastern Brazil). *Journal of South American*
678 *Earth Science* 2, 191-198.

679 Rhodes, A.N., 1998. A Method for the Preparation and Quantification of Microscopic Charcoal
680 from Terrestrial and Lacustrine Sediment Cores. *The Holocene* 8(1), 113-17.

681 Rull, V., Vegas-Vilarrúbia, T., Nogué, S., Huber, O., 2009. Conservation of the unique
682 neotropical vascular flora of the Guyana Highlands in the face of global warming.
683 *Conservation Biology* 23, 1323e1327.

684 RStudio Team, 2016. RStudio: Integrated Development for R. RStudio, Inc., Boston, MA url:
685 <http://www.rstudio.com/>.

686 Safford, H. D., 1999a. Brazilian Páramos I. An introduction to the physical environment and
687 vegetation of the *campos de altitude*. *Journal of Biogeography* 26, 693-712.

688 Safford, H.D., 1999b. Brazilian Páramos II. Macro- and mesoclimate of the campos de altitude
689 and affinities with high mountain climates of the tropical Andes and Costa Rica. *Journal of*
690 *Biogeography* 26, 713-737.

691 Safford, H.D., 2001. Brazilian Páramos III. Patterns and rates of postfire regeneration in the
692 campos de altitude. *Biotropica* 33(2), 282-302.

693 Safford, H.D., 2007. Brazilian Páramos IV. Phytogeography of the campos de altitude. *Journal of*
694 *Biogeography* 34, 1701-1722.

695 Safford, H. D., Hayward, G., Heller, N., Wiens, J.A., 2012. Climate change and historical
696 ecology: can the past still inform the future? Pp. 46-62, in: J. A. Wiens, G. Hayward, H. D.
697 Safford, and C.M. Giffen (eds). *Historical environmental variation in conservation and*
698 *natural resource management*. John Wiley and Sons, New York, NY.

699 Scheel-Ybert, R., 2001. Man and Vegetation in Southeastern Brazil during the Late Holocene.
700 *Journal of Archaeological Science* 28, 471-480.

701 Scheer, M. B., Mochinski, A. Y., 2009. Florística vascular da Floresta Ombrófila Densa
702 Altomontana de quarta serra no Paraná. *Biota Neotrop.* 9(2), 51-69.

703 Stevenson, J., Haberle, S., 2005. Macro Charcoal Analysis: a modified technique used by the
704 department of Archaeology and Natural History. *Palaeoworks Technical Papers* 5, p. 7.
705 Department of Archaeology and Natural History, Research School of Pacific and Asian
706 Studies, coombs Building, Australian National University, ACT 0200, Australia.

707 Stockmarr, J., 1971. Tablets with Spores used in Absolute Pollen Analysis. *Pollen et Spores* 13,
708 615 – 621.

709 Stuiver, M., Reimer, P.J., and Reimer, R.W., 2019. CALIB 7.1 at <http://calib.org>.

710 Vegas-Vilarrúbia, T., Rull, V., Montoya, E., Safont, E., 2011. Quaternary palaeoecology and
711 nature conservation: a general review with examples from the neotropics. *Quaternary*
712 *Science Reviews* 30, 2361-2388.

713 Veríssimo, P.N., Safford, H.D., Behling, H., 2012. Holocene vegetation and fire history of the
714 Serra do Caparaó, SE Brazil. *The Holocene* 22, 1243-1250.

715 Vuille, M., Burns, S.J., Taylor, B.L., Cruz, F.W., Bird, B.W., Abbot, M.B., Kanner, L.C., Cheng,
716 H., Novello, V.F., 2012. A review of the South American monsoon history as recorded in
717 stable isotopic proxies over the past two millennia. *Clim. Past.* 8, 1309-1321.

718 Whitlock, C., Skinner, C.N., Bartlein, P.J., Minckley, T., Mohr, J.A., 2004. Comparison of

719 charcoal and tree-ring records of recent fires in the eastern Klamath Mountains, California,
 720 USA. Canadian Journal of Forest Research 34, 2110-2121.

721

722 **SUPPLEMENTARY MATERIAL**

723 *List of taxa identified in the VAF sediment.*

Taxa	Subgroup	Group	Pollination
Asteraceae	Asteraceae	CDA	Entomophily
<i>Ambrosia</i>	Asteraceae	CDA	Entomophily
<i>Baccharis</i>	Asteraceae	CDA	Entomophily
<i>Jungia</i>	Asteraceae	CDA	Entomophily
<i>Senecio</i>	Asteraceae	CDA	Entomophily
<i>Vernonia</i>	Asteraceae	CDA	Entomophily
<i>Alstromeria</i>	Herbs & Shrubs	CDA	Entomophily
Amaranthaceae/Chenopodiaceae	Herbs & Shrubs	CDA	Entomophily
Apiaceae	Herbs & Shrubs	CDA	Entomophily
<i>Borreria</i>	Herbs & Shrubs	CDA	Entomophily
Ericaceae	Herbs & Shrubs	CDA	Entomophily
<i>Eriocaulon</i>	Herbs & Shrubs	CDA	Anemophily/Entomophily
<i>Eryngium</i> type 1	Herbs & Shrubs	CDA	Entomophily
<i>Eryngium</i> type2	Herbs & Shrubs	CDA	Entomophily
Fabaceae	Herbs & Shrubs	CDA	Entomophily/Aviphily
<i>Hippeastrum</i>	Herbs & Shrubs	CDA	Entomophily
<i>Hypericum</i>	Herbs & Shrubs	CDA	Entomophily
<i>Hyptis</i>	Herbs & Shrubs	CDA	Entomophily/Aviphily
Lamiaceae	Herbs & Shrubs	CDA	Entomophily/Aviphily
Malphiaceae	Herbs & Shrubs	CDA	Entomophily
Malvaceae	Herbs & Shrubs	CDA	Entomophily
Poaceae	Herbs & Shrubs	CDA	Anemophily
<i>Polygala</i>	Herbs & Shrubs	CDA	Entomophily
Ranunculaceae	Herbs & Shrubs	CDA	Anemophily/Entomophily
<i>Ripsalis</i>	Herbs & Shrubs	CDA	Entomophily/Aviphily
Scrophulariaceae	Herbs & Shrubs	CDA	Entomophily
<i>Spermacoce</i>	Herbs & Shrubs	CDA	Entomophily
<i>Valeriana</i>	Herbs & Shrubs	CDA	Entomophily
Cyperaceae	Aquatics	CDA	Anemophily
<i>Hydrocotyle</i>	Aquatics	CDA	Entomophily
Liliaceae/Amaryllidaceae	Aquatics	CDA	Entomophily
<i>Typha</i>	Aquatics	CDA	Anemophily
<i>Xyris</i>	Aquatics	CDA	Anemophily
<i>Allophylus</i>	UMARF		Entomophily
<i>Begonia</i>	UMARF		Entomophily
<i>Clethra</i>	UMARF		Entomophily
<i>Croton</i>	UMARF		Entomophily
<i>Daphnopsis</i>	UMARF		Entomophily
<i>Drymis</i>	UMARF		Entomophily/Aviphily
<i>Fuchsia</i>	UMARF		Aviphily
<i>Griselinia</i>	UMARF		Entomophily
<i>Hedyosmum</i>	UMARF		Anemophily/Entomophily

<i>Ilex</i>	UMARF		Anemophily/Entomophily
<i>Laplacea</i>	UMARF		Entomophily
<i>Mimosa scabrella</i>	UMARF		Entomophily/Aviphily
<i>Myrsine</i>	UMARF		Anemophily
<i>Ouratea</i>	UMARF		Entomophily
<i>Podocarpus</i>	UMARF		Entomophily
<i>Roupala</i>	UMARF		Entomophily/Aviphily
<i>Struthanthus</i>	UMARF		Entomophily
<i>Styrax</i>	UMARF		Entomophily
<i>Symplocos lanceolata</i>	UMARF		Entomophily
<i>Symplocos tenuifolia</i>	UMARF		Entomophily
<i>Weinmannia</i>	UMARF		Entomophily/Aviphily
<i>Alseis floribunda</i>	OARF		Entomophily
Araliaceae	OARF		Entomophily
Bignoniaceae	OARF		Entomophily/Aviphily
<i>Celtis</i>	OARF		Anemophily
<i>Coccocypselum</i>	OARF		Entomophily
<i>Dodonea</i>	OARF		Anemophily
Euphorbiaceae	OARF		Entomophily
Flacourtiaceae	OARF		Entomophily/Aviphily
<i>Lamanonia</i>	OARF		Entomophily
<i>Matayba</i>	OARF		Entomophily
Melastomataceae	OARF		Entomophily
Meliaceae	OARF		Entomophily
<i>Meliosma</i>	OARF		Entomophily
Menispermaceae	OARF		Entomophily
Mimosaceae	OARF		Anemophily/Entomophily/Aviphily
Myrtaceae	OARF		Entomophily/Aviphily
<i>Oreopanax</i>	OARF		Entomophily
<i>Pera</i>	OARF		Entomophily
<i>Piper</i>	OARF		Anemophily/Entomophily
<i>Prockia</i>	OARF		Entomophily/Aviphily
<i>Prunus</i> type	OARF		Entomophily
Rubiaceae	OARF		Entomophily
Sapindaceae	OARF		Entomophily
<i>Schefflera</i>	OARF		Entomophily
<i>Sebastiania brasiliensis</i>	OARF		Anemophily
<i>Sebastiania commersoniana</i>	OARF		Anemophily
<i>Solanum</i>	OARF		Entomophily
<i>Trema</i>	OARF		Anemophily
<i>Urvillea</i>	OARF		Entomophily
<i>Vochysia</i>	OARF		Aviphily/Entomophily/Monkeys
<i>Alchornea</i>	LARF		Anemophily/Entomophily
<i>Cecropia</i>	LARF		Anemophily/Entomophily
<i>Euterpe/Geonoma</i>	LARF		Entomophily
<i>Hyeronima</i>	LARF		Entomophily
Moraceae/Urticaceae	LARF		Anemophily
<i>Rhamnus</i> type	LARF		Entomophily
Sapotaceae	LARF		Entomophily/Quiropterophily
<i>Virola</i>	LARF		Entomophily
<i>Alsophila</i>	Tree fern		Hydrophily
<i>Cyathea psilate</i>	Tree fern		Hydrophily
<i>Cyathea reticulata</i>	Tree fern		Hydrophily

<i>Cyathea verrucate</i>	Tree fern		Hydrophily
<i>Dicksonia</i>	Tree fern		Hydrophily
<i>Lophosoria quadripinnata</i>	Tree fern		Hydrophily
<i>Nephelea</i>	Tree fern		Hydrophily
<i>Anemia phyllitides</i>	Spore		Hydrophily
<i>Hymenophyllum</i>	Spore		Hydrophily
<i>Lycopodium clavatum</i>	Spore		Hydrophily
<i>Lycopodium</i> foveolate form type	Spore		Hydrophily
Monolete clavate	Spore		Hydrophily
Monolete echinate	Spore		Hydrophily
Monolete psilate	Spore		Hydrophily
Monolete psilate large	Spore		Hydrophily
Monolete scabrate	Spore		Hydrophily
Monolete striate	Spore		Hydrophily
Monolete with perispore	Spore		Hydrophily
<i>Osmunda</i>	Spore		Hydrophily
<i>Phaeoceros</i>	Spore		Hydrophily
<i>Pityrogramma</i>	Spore		Hydrophily
Polypodiaceae	Spore		Hydrophily
Pteridophyta type 4	Spore		Hydrophily
Pteridophyta type 7	Spore		Hydrophily
<i>Pteris</i> type	Spore		Hydrophily
<i>Sellaginella excurrentis</i> type	Spore		Hydrophily
<i>Sphagnum</i>	Spore		Hydrophily
Trilete clavate	Spore		Hydrophily
Trilete psilate	Spore		Hydrophily
Trilete scabrate	Spore		Hydrophily
Trilete striate	Spore		Hydrophily
Trilete verrucate	Spore		Hydrophily
Trilete with perispore	Spore		Hydrophily